A robust inlier identification algorithm for point cloud registration via ℓ_0-minimization

Yinuo Jiang[1,*] Xiuchuan Tang[2,*] Cheng Cheng[1] Ye Yuan[1,†]

[1]Huazhong University of Science and Technology [2] Tsinghua University

NEURAL INFORMATION PROCESSING SYSTEMS

Motivation and contributions

Background: Point cloud registration is a fundamental task in vision and robotics, e.g., 3D reconstruction and autonomous driving.

Motivation: Correspondences in point cloud registration are prone to outliers, significantly reducing registration accuracy and highlighting the need for precise inlier identification.

Key Contributions:

- A novel robust inlier identification algorithm is proposed by reformulating the conventional registration as an alignment error ℓ_0-minimization problem.
- A two-stage decoupling strategy is designed to effectively solve the proposed ℓ_0-minimization problem based on the Bayes Theorem.

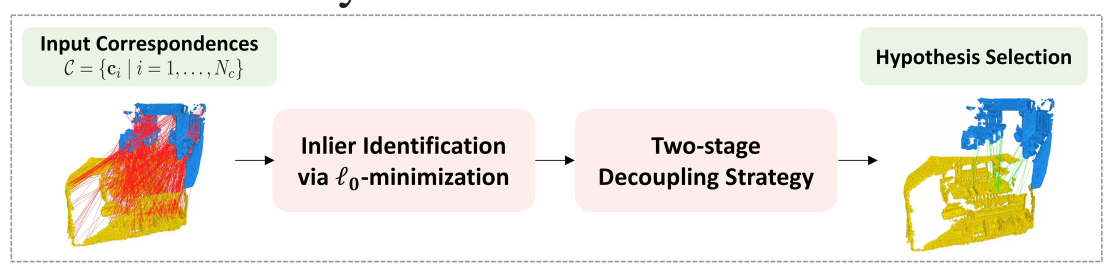

Problem formulation

Main idea: We reformulat the conventional registration as an alignment error ℓ_0-minimization problem

- The conventional registration problem:

$$\min_{\mathbf{R},\mathbf{t}} \sum_{(\mathbf{p}_i,\mathbf{q}_i)\in\mathcal{C}} \|\mathbf{q}_i - \mathbf{R}\mathbf{p}_i - \mathbf{t}\|_2^2 \,, \qquad (1)$$

where $\mathcal{C} = \{\mathbf{c}_i \mid i = 1, \ldots, N_c\}$ is the initial correspondence set.

- Considering only inliers can be fitted by the same transformation, the optimal transformation is estimated as the one that fits the largest number of inliers. Our optimization objective is to maximize the count of zero vectors in the alignment error via ℓ_0 norm:

$$\mathbf{O}^* = \arg\min_{\mathbf{O}} \|\mathbf{O}\|_{\ell_0} \,, \quad \text{subject to: } \mathbf{o}_i = \mathbf{q}_i - \mathbf{R}\mathbf{p}_i - \mathbf{t} - \xi_k \,, \qquad (2)$$

where $\mathbf{O} = [\mathbf{o}_1, \mathbf{o}_2, \ldots, \mathbf{o}_{N_c}]$ is the alignment error matrix and and ξ_k is the Gaussian noise.

Robustness to outliers and noise

We evaluate the robustness and accuracy of our algorithm using the Bunny point cloud from the Stanford 3D Scan Repository. To evaluate robustness against outliers, we increase the outlier ratio from 91% to 99%. For robustness to noise, we increase the noise standard deviation from $\sigma = 0.01$ to $\sigma = 0.09$.

Robustness to outliers:

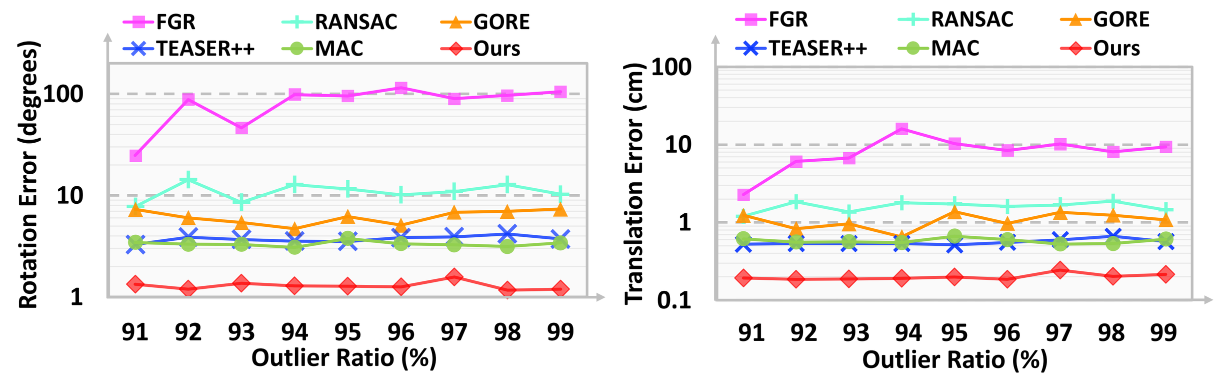

Robustness to noise:

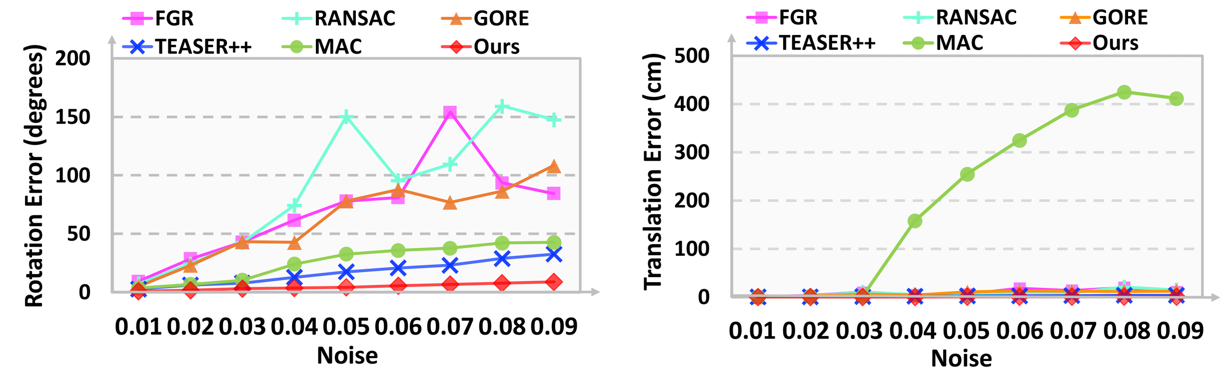

Algorithm

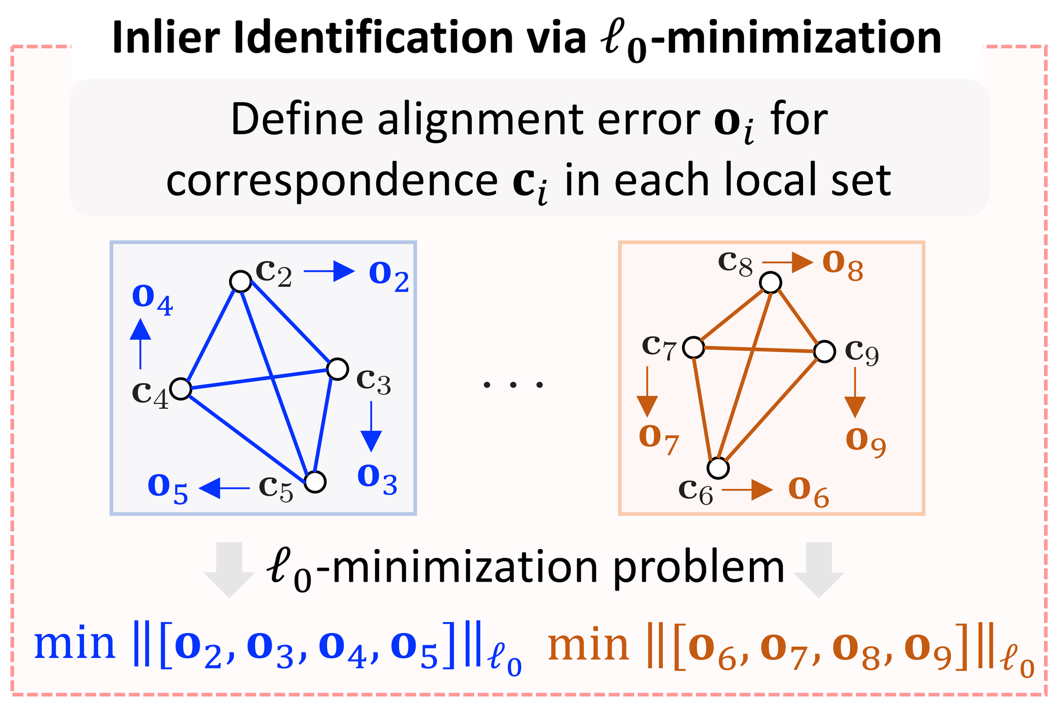

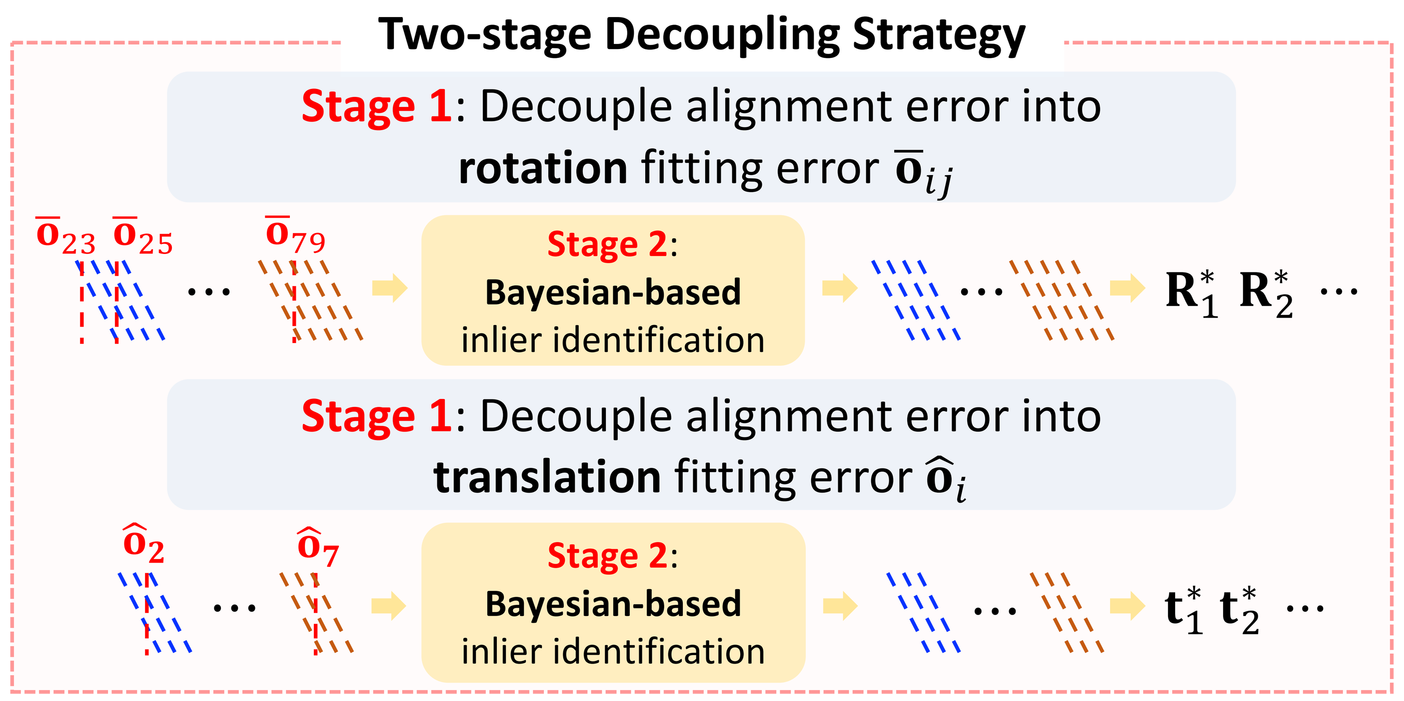

Inlier Identification via ℓ_0-minimization

We identify compatible correspondences to form local sets. For correspondences in the k-th local set, the ℓ_0-minimization problem is defined as:

$$\mathbf{O}_k^* = \arg\min_{\mathbf{O}_k} \|\mathbf{O}_k\|_{\ell_0} \,, \quad \text{subject to: } \mathbf{O}_k = \mathbf{Q}_k - \mathbf{P}_k\mathbf{R}_k - \mathbf{t}_k\mathbf{1}^T - \mathbf{\Xi}_k \,. \qquad (3)$$

Two-stage Decoupling Strategy

- **Stage 1:** For any two given points $\mathbf{p}_{k_i}$ and $\mathbf{q}_{k_j}$ in the k-th local set, the translation vector $\mathbf{t}_k$ cancels out in the subtraction:

$$\mathbf{q}_{k_j} - \mathbf{q}_{k_i} = \mathbf{R}_k\left(\mathbf{p}_{k_j} - \mathbf{p}_{k_i}\right) + \left(\mathbf{o}_{k_j} - \mathbf{o}_{k_i}\right) + \left(\xi_{k_j} - \xi_{k_i}\right) \qquad (4)$$

  This leads to two separate ℓ_0-minimization problems for fitting rotation and translation errors.

- **Stage 2:** We introduce null-space matrices to isolate rotation and translation in the ℓ_0-minimization constraints, where $\bar{\mathbf{\Theta}}_k\bar{\mathbf{P}}_k = \mathbf{0}$ and $\mathbf{\Theta}_k\mathbf{1} = \mathbf{0}$.
Based on the Bayes Theorem and Maximum A Posteriori (MAP) estimate, the unconstrained optimization problems for rotation and translation fitting are formulated as:

$$\min_{\bar{\mathbf{O}}_k} \frac{1}{2}\left\|(\tilde{\bar{\mathbf{Q}}}_k - \bar{\mathbf{\Theta}}\bar{\mathbf{O}}_k)^T\bar{\mathbf{\Pi}}_k^{-1}(\tilde{\bar{\mathbf{Q}}}_k - \bar{\mathbf{\Theta}}_k\bar{\mathbf{O}}_k)\right\|_F^2 + \lambda_R\|\bar{\mathbf{O}}_k\|_{\ell_0}^2 \,, \qquad (5)$$

where $\tilde{\bar{\mathbf{Q}}}_k = \bar{\mathbf{\Theta}}_k\bar{\mathbf{Q}}_k$ and $\bar{\mathbf{\Theta}}_k\bar{\mathbf{\Theta}}_k^T = \bar{\mathbf{\Pi}}_k$.

$$\min_{\hat{\mathbf{O}}_k} \frac{1}{2}\left\|(\mathbf{X}_k - \mathbf{\Theta}_k\hat{\mathbf{O}}_k^T)^T\mathbf{\Pi}_k^{-1}(\mathbf{X}_k - \mathbf{\Theta}_k\hat{\mathbf{O}}_k^T)\right\|_F^2 + \lambda_t\left\|\hat{\mathbf{O}}_k\right\|_{\ell_0}^2 \,, \qquad (6)$$

where $\mathbf{X}_k = \mathbf{\Theta}_k(\mathbf{Q}_k^T - (\mathbf{P}_k\mathbf{R}_k^*)^T)$ and $\mathbf{\Pi}_k = \mathbf{\Theta}_k\mathbf{\Theta}_k^T$.
Explicit solutions $\bar{\mathbf{O}}_k^*$ and $\hat{\mathbf{O}}_k^*$ can be directly computed due to convex relaxation via the Frobenius norm:

$$\bar{\mathbf{O}}_k^* = (\bar{\mathbf{\Theta}}_k^T\bar{\mathbf{\Pi}}_k^{-1}\bar{\mathbf{\Theta}}_k + 2\lambda_R\mathbf{I})_k^{-1}\bar{\mathbf{\Theta}}_k^T\bar{\mathbf{\Pi}}_k^{-1}\tilde{\bar{\mathbf{Q}}}_k \,.$$
$$\hat{\mathbf{O}}_k^* = ((2\lambda_t\mathbf{I} + \mathbf{\Theta}_k^T\mathbf{\Pi}_k^{-1}\mathbf{\Theta}_k)^{-1}\mathbf{\Theta}_k^T\mathbf{\Pi}_k^{-1}\mathbf{X}_k)^T \,. \qquad (7)$$

Experiments

Comparisons on the 3DMatch dataset:

	FPFH			FCGF			3DSmoothNet			Time(s)
	RR(%)↑	RE(°)↓	TE(cm)↓	RR(%)↑	RE(°)↓	TE(cm)↓	RR(%)↑	RE(°)↓	TE(cm)↓	
i) Traditional										
FGR	40.91	4.96	10.25	78.93	2.90	8.41	73.26	2.51	7.45	0.89
RANSAC	66.10	3.95	11.03	91.44	2.69	8.38	92.30	2.59	7.91	2.86
TEASER++	75.48	2.48	7.31	85.71	2.73	8.66	92.05	2.23	6.62	0.03
SC^2-PCR	83.90	2.12	6.69	93.16	2.06	6.53	94.82	1.76	5.98	0.12
MAC	83.90	**2.11**	6.80	**93.72**	**2.04**	6.54	94.57	2.21	6.52	5.54
TR-DE	-	-	-	-	-	-	91.37	2.71	7.62	-
TEAR	-	-	-	-	-	-	94.52	2.06	6.55	-
ii) Deep learned										
DGR	32.84	2.45	7.53	88.85	2.28	7.02	-	-	-	1.53
PointDSC	72.95	2.18	**6.45**	91.87	2.10	6.54	93.65	2.17	6.75	0.10
VBReg	82.57	2.14	6.77	93.53	**2.04**	6.49	37.09	6.15	15.65	0.20
Ours	**83.92**	2.12	6.64	93.28	**2.04**	**6.48**	**95.07**	**1.75**	**5.97**	0.36

Comparisons on the KITTI dataset:

	FPFH			FCGF			Time(s)
	RR(%)↑	RE(°)↓	TE(cm)↓	RR(%)↑	RE(°)↓	TE(cm)↓	
i) Traditional							
FGR	5.23	0.86	43.84	89.54	0.46	25.72	3.88
RANSAC	74.41	1.55	30.20	80.36	0.73	26.79	5.43
TEASER++	91.17	1.03	17.98	95.51	0.33	22.38	0.03
SC^2-PCR	99.46	0.35	7.87	98.02	0.33	20.69	0.31
MAC	97.66	0.41	8.61	97.84	0.34	19.34	3.29
TR-DE	96.76	0.90	15.63	**98.20**	0.38	**18.00**	-
TEAR	99.10	0.39	8.62	-	-	-	-
ii) Deep learned							
DGR	77.12	1.64	33.10	96.90	0.34	21.70	2.29
PointDSC	98.92	0.38	8.35	97.84	0.33	20.32	0.45
VBReg	98.92	0.45	8.41	98.02	0.32	20.91	0.24
Ours	**99.56**	**0.34**	**7.85**	**98.20**	**0.32**	20.73	0.54

Comparisons on the 3DLoMatch dataset:

	5000	2500	1000	500	250
	Predator				
FGR	36.4	38.2	39.7	39.6	38.0
RANSAC	62.3	62.8	62.4	61.5	58.2
TEASER++	62.9	62.6	61.9	59.0	56.7
SC^2-PCR	68.9	68.4	68.7	67.1	64.9
MAC	69.4	69.3	68.4	**67.7**	64.6
TR-DE	64.0	64.8	61.7	58.8	56.5
PointDSC	68.1	67.3	66.5	63.4	60.5
VBReg	**69.9**	69.8	68.7	66.4	63.0
Ours	**69.9**	**69.9**	**69.2**	**67.7**	**65.0**

Qualitative results on the 3DMatch dataset:

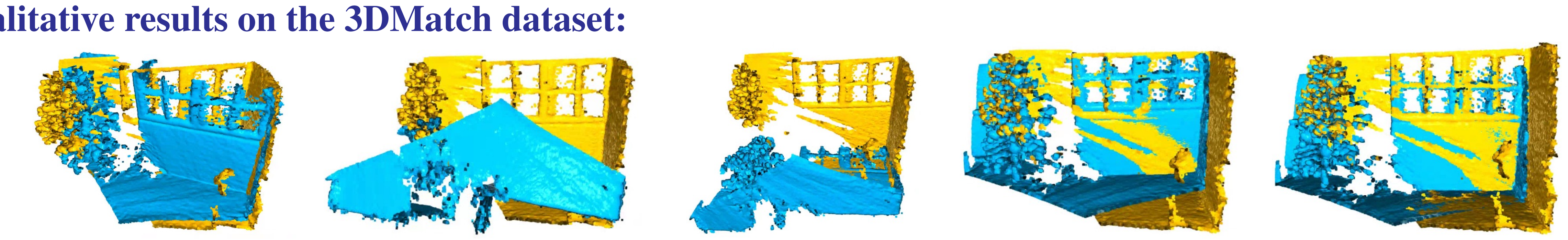

(a) Input (b) MAC (c) SC^2-PCR (d) Ours (e) Ground-truth